Application of Multiobjective Optimization in the Design and Operation of Reactive SMB and Its Experimental Verification

Weifang Yu, K. Hidajat, and Ajay K. Ray*

Department of Chemical and Environmental Engineering, National University of Singapore, 10 Kent Ridge Crescent, Singapore 119260

The performance of reactive simulated moving bed (SMBR) process was optimized for an experimentally verified mathematical model for the synthesis of methyl acetate ester. Multiobjective optimization was performed for an existing SMBR experimental setup, and optimum results obtained were subsequently verified experimentally. Thereafter, few other multiobjective optimization studies were performed for both existing setup and at the design stage. The effect of variable (distributed) feed flow rate on the optimum performance of SMBR was also investigated. The optimization was performed using AI-based nondominated sorting genetic algorithm (NSGA), which resulted in Pareto optimal solutions. The paper demonstrates usefulness of multiobjective optimization in the design of reactive SMB processes.

Introduction

The simulated moving bed (SMB)[1] is a practical way to implement continuous countercurrent operation of chromatographic separation processes. In SMB technology, the countercurrent movement of the fluid phase toward the solid phase is mimicked by switching the introduction and withdrawal ports periodically and simultaneously along a series of fixed columns in the direction of the fluid flow. For ease of operation, the columns are actually divided into sections (or zones). The number of columns within each section and the total number of columns are adjustable depending on the design of the system for any particular applications. SMB also provides opportunities for coupling reactions,[2−4] which allow higher conversion for equilibrium-limited reversible reactions by on-site separation of the products, which leads to better yield and selectivity compared to typical fixed-bed processes. Additionally, the combination of two unit operations in one single apparatus reduces capital and operating cost. However, such integration of chemical reaction and separation complicates the process design and plant operation. The optimal design and determination of optimal operating parameters, such as switching time, flow rates in each section, and length of each column and its distribution, are therefore essential to evaluate the economic potential of such processes and to successfully implement reactive SMB processes on industrial scale.

The modeling, simulation, and experimental study of SMBR for the synthesis of methyl acetate (MeOAc) have been carried out details of which are reported elsewhere.[5,6] A rigorous mathematical model was developed to describe the dynamic behavior of SMBR for the synthesis of MeOAc. The numerical simulation results were then compared with the experimental results to validate the model.[6] Thereafter, a parametric sensitivity study was performed to investigate the effects of several design and operating parameters, such as switching time, number of columns in each section, and inlet and outlet flow rates, on the performance of SMBR. It was found that there is a complex interplay of these parameters and some of the operating variables not only influence the yield, selectivity, and purity of MeOAc significantly but also act in conflicting ways.[6] This means any desirable change in one objective function (e.g., yield) results in an unfavorable change in another objective function (e.g., purity). In other words, it is not possible to improve yield and purity of MeOAc simultaneously as when one is improved, the other is worsened. Although several studies[7−10] have been reported on the design and optimization of SMBR, they only involved single objective optimization, which is usually not sufficient for the real-life design of complex reactive SMB systems. Therefore, a more realistic approach, multiobjective optimization,[11] is necessary for the design of reactive SMB process. In this study, multiobjective optimization is used for the design of reactive SMB for the methyl acetate synthesis. Subsequently, some of the optimal solutions obtained from the optimization studies were verified experimentally to ascertain out whether optimum results can be achieved.

The principle of multicriterion optimization with conflicting objectives is different from that of single objective optimization.[11] Instead of trying to find the best design solution, which is usually the global optimum, the goal of multiobjective optimization is to obtain a set of equally good solutions, which are known as Pareto optimal solutions. In a set of Pareto optimal solutions, no solution can be considered to be better than any other solutions with respect to all objective functions. When one moves from one Pareto solution to other, at least one objective function improve while at least one other worsened. So the selection of any optimal solution from a Pareto set will depend on auxiliary information. However, by narrowing down the choices, the Pareto sets does provide decision makers with useful guidance in selecting the desired operating conditions (the preferred solution) from among the (restricted) set of Pareto optimal solutions, rather than from a much larger number of possibilities.

In earlier years, multiobjective optimization problems were usually solved using a single *scalar* objective function, which was a weighted-average of the several

* To whom correspondence should be addressed. Fax: +65 6779 1936. E-mail: cheakr@nus.edu.sg.

10.1021/ie030387p CCC: $25.00
Published on Web 11/19/2003

objectives ("scalarization" of the vector objective function). This process allows a simpler algorithm to be used, but unfortunately, the solution obtained depends largely on the values assigned to the weighting factors used, which is done quite arbitrarily. An even more important disadvantage of the scalarization of the several objectives is that the algorithm may miss some optimal solutions, which can never be found, regardless of the weighting factors chosen. This happens if the nonconvexity of the objective function gives rise to a duality gap.[12] Several methods are available to solve multiobjective optimization problems, e.g., the ϵ-constraint method, goal attainment method, and different adaptations of the nondominated sorting genetic algorithm (NSGA).[11−13]

In this paper, a comprehensive multiobjective optimization study of reactive SMB processes is performed using the nondominated sorting genetic algorithm (NSGA)[12,14] in obtaining Pareto optimal solutions. Genetic algorithms are nontraditional search and optimization methods based on the mechanics of natural genetics and natural selection.[15] Indeed, different versions (adaptations) of NSGA[12] have been applied in recent years to optimize several processes of industrial importance in chemical engineering[11] and, in particular, chemical reaction engineering.[14] This technique offers several advantages,[11−12] as for example: (a) its efficiency is relatively insensitive to the shape of the Pareto optimal front, (b) problems with uncertainties, stochasticities, and with discrete search spaces can be handled efficiently, (c) the "spread" of the Pareto set obtained is excellent (in contrast, the efficiency of other optimization methods decides the spread of the solutions obtained), and (d) it involves a single application to obtain the entire Pareto set (in contrast to other methods, e.g., the ϵ-constraint method, which needs to be applied several times over).

Initially, the optimal solutions in terms of maximization of purity and yield of MeOAc for an existing SMBR experimental unit were obtained. Subsequently, experiments were performed at the predicted optimal operating conditions and the performances of the reactor were compared. This not only demonstrates that the model is robust, but also shows that optimization results can be duplicated experimentally. Subsequently, the effects of constant and nonuniform (distributed) feed flow rate and total number of columns on the Pareto optimal solutions for few different combinations of two and three objective functions were investigated. This paper illustrates a realistic approach toward the optimal design and operation of reactive SMB systems.

Mathematical Model of Reactive SMB Systems

A schematic diagram of a six-column SMBR unit is illustrated in Figure 1. The two incoming streams (feed and eluent) and the two outgoing streams (raffinate and extract) divide the system into four sections, namely P, Q, R and S, each of which consisting of p, q, r, and s columns, respectively. The flow rate in section P (feed section), Q_P, was chosen as the reference flow rate based on which all other flow rates were described. The ratios of the feed flow rate, F, the raffinate flow rate, Ra, the eluent flow rate, E, to that in section P (Q_P) were designated as α, β, and γ, respectively. By advancing the introduction and withdrawal ports simultaneously,

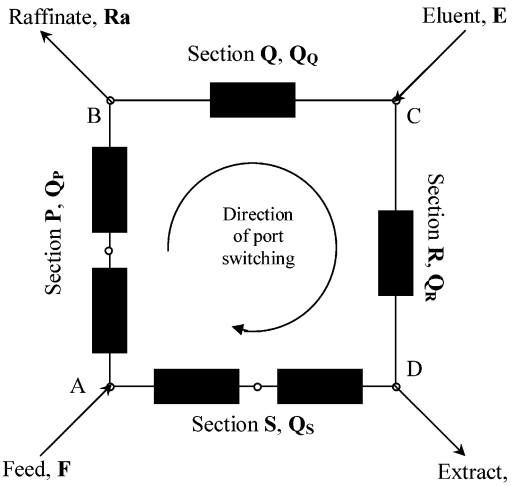

Figure 1. Schematic diagram of a six-column SMBR system. The inlets and outlets divide the entire system into four sections: P, Q, R, and S with 2, 1, 1 and 2 columns, respectively. The flow rates in each section is given by $Q_Q = (1 - \beta)Q_P$, $Q_R = (1 - \beta + \gamma)Q_P$, and $Q_S = (1 - \alpha)Q_P$, where α, β, and γ are given by F/Q_P, Ra/Q_P, E/Q_P.

column by column, in the direction of fluid flow at a predetermined time interval (switching time, t_s), the simulation of countercurrent movement of the solid-phase toward the fluid phase is achieved. In SMBR, switching time and column configuration (the number of columns in each section) are decided a priori and are kept constant throughout the entire operation.

The experimentally verified mathematical model describing the dynamic behavior of SMBR for the synthesis of MeOAc was developed and is described in detail elsewhere.[6] The same is not discussed here for brevity, but for completeness, complete sets of equations are provided in Appendix. The mass balance equation (eq A1), initial (eqs A4−A6), and boundary (eqs A7−A10) conditions, kinetic equation (eq A2), and adsorption isotherm (eq A3) completely define the SMBR system. The PDEs were solved using method of lines.[16] The PDEs were first discretized in space using five-point centered and biased upwind approximations for the derivatives[16] to convert it into a set of several-coupled ODE-IVPs and the resultant stiff ODEs of the initial value kind were solved using the subroutine DIVPAG (which is based on Gear's backward differentiation formulas) in the IMSL library. Since periodic switching is imposed on the system, the reactor works under transient conditions. Whenever switching is performed a new initial value problem must be solved. However, a cyclic (periodic) steady state with a period equal to the switching time is eventually attained. After each switching, column numbering was redefined according to eq A11 so that feed is always introduced into the first column. The mathematical model described is solved using experimentally determined adsorption and kinetic parameters[5] given in Appendix for the MeOAc synthesis reaction. The model can predict the concentration profiles of the limiting reactant (HOAc) and products (MeOAc and H_2O). It was observed that the SMBR configuration reaches a pseudo-steady state after 60 switching operation and enhancement of yield and selectivity of MeOAc is possible due to the separation of the products at the site reaction. The CPU time for one simulation run (to reach cyclic steady state) takes 0.2 s on a Cray J916 supercomputer.

A set of objective functions examined in this work are defined as follows:

$$X_{\mathrm{HOAc}} = \frac{(\text{HOAc fed} - \text{HOAc collected at raffinate and extract})}{\text{HOAc fed}} = \frac{\alpha C_{\mathrm{HOAc,F}} t_s - [\beta \cdot \int_0^{t_s} C^{(N)}_{\mathrm{HOAc,p}}|_{z=L_{\mathrm{col}}} \mathrm{d}t + (\alpha + \gamma - \beta)\int_0^{t_s} C^{(N)}_{\mathrm{HOAc,p+q+r}}|_{z=L_{\mathrm{col}}} \mathrm{d}t]}{\alpha C_{\mathrm{HOAc,F}} t_s} \quad (1)$$

$$Y_{\mathrm{MeOAc}} = \frac{\text{MeOAc collected in raffinate}}{\text{HOAc fed}} = \frac{\beta[\int_0^{t_s} C^{(N)}_{\mathrm{MeOAc,p}}|_{z=L_{\mathrm{col}}} \mathrm{d}t]}{\alpha C_{\mathrm{HOAc,F}} t_s} \quad (2)$$

$$P_{\mathrm{MeOAc}} = \frac{\text{MeOAc collected in raffinate}}{[\mathrm{MeOAc} + \mathrm{H_2O} + \mathrm{HOAc}]\ \text{collected in raffinate}} = \frac{\int_0^{t_s} C^{(N)}_{\mathrm{MeOAc,p}}|_{z=L_{\mathrm{col}}} \mathrm{d}t}{\int_0^{t_s} (C^{(N)}_{\mathrm{MeOAc,p}} + C^{(N)}_{\mathrm{H_2O,p}} + C^{(N)}_{\mathrm{HOAc,p}})|_{z=L_{\mathrm{col}}} \mathrm{d}t} \quad (3)$$

$$S_{\mathrm{MeOAc}} = \frac{\text{MeOAc collected in raffinate}}{[\mathrm{MeOAc} + \mathrm{H_2O}]\ \text{collected in raffinate}} = \frac{\int_0^{t_s} C^{(N)}_{\mathrm{MeOAc,p}}|_{z=L_{\mathrm{col}}} \mathrm{d}t}{\int_0^{t_s} (C^{(N)}_{\mathrm{MeOAc,p}} + C^{(N)}_{\mathrm{H_2O,p}})|_{z=L_{\mathrm{col}}} \mathrm{d}t} \quad (4)$$

$$V_{\mathrm{solid}} = N^{\pi}/_4 (d_{\mathrm{col}})^2 (1 - \epsilon) \quad (5)$$

The effect of switching time (t_s), number of columns (p, q, r, and s) in sections P, Q, R, and S, respectively, and feed (α), product (β), solvent (γ) and reference (Q_P) flow rates (see Figure 1) were studied on the yield, selectivity, purity of MeOAc, and conversion of the limiting reactant, acetic acid (HOAc). The detailed sensitivity analysis of these parameters is discussed elswhere.[6] It was observed that switching time and solvent flow rate play a crucial role in achieving effective separation between the components. It was found that some of the process parameters not only alter the yield, selectivity and purity of MeOAc profoundly but also act in conflicting manner. For example, parameters such as β and γ have conflicting influence on the yield and purity (or selectivity) of MeOAc. Furthermore, depending on t_s, the effect of α, β, γ, and p are quite different. The influence of t_s is particularly complex. Its optimum value depend not only on the distribution of columns in sections P and S, but also on the value of α, β, and γ. It is not possible to maximize yield and selectivity simultaneously. One must perform multiobjective optimization to determine optimal conditions and configuration of SMBR. It is evident that optimum process design for SMBR is not only time-consuming but almost impossible to obtain just by simulation due to a large number of parameters, which are interrelated and at times conflicting. A systematic multiobjective optimization study can not only provide optimum operating conditions for the desired objectives but also will be helpful in understanding the roles of each parameter in the SMBR system.

Optimization of Reactive SMB Process

The optimization problems of reactive SMB process may be classified into two main categories, namely, the performance enhancement of an existing unit and the optimal design of a new plant. The process can be optimized for different objectives, which may include minimization of fixed cost (e.g., equipment such as length, diameter and number of columns, i.e., volume of stationary phase) or operating cost (e.g., desorbent flow rates and/or temperature), and/or maximization of throughput (e.g., feed flow rate) or product quality (e.g., purity of product streams). Since cost data is site (location) as well as time specific, it may not always be a meaningful objective function. In SMBR, unlike SMB process for separation only (like chiral separation or *p*-xylene recovery in Parex process), there is usually only one desired product, which is withdrawn either from the raffinate or the extract port. Hence, in reactive SMB, objectives usually include maximization of yield, purity or selectivity of the desired product and/or the conversion of the limiting reactant. One can also consider objective functions such as maximization of throughput (capacity) or minimization of desorbent (eluent) flow rate. It is possible to consider all these objective functions together, but it may be difficult to analyze the optimum solutions, as one has to consider multidimensional surfaces. It should be noted that a Pareto point is defined as when one moves from one point to another at least one objective function improve while at least one worsens. Hence, for a three objective function optimization, when one move from one Pareto point to another there are two distinct possibilities: (a) two objective functions improve while one deteriorates, or (b) one objective function get better while two others get worse. Hence, analysis requires multidimensional surfaces, which not necessarily are smooth, and therefore, requires determination of many optimal solutions for creating the surface.

Table 1. Computational Parameters of NSGA Used in This Work

no. of generation, N_{gen}	50
population size, N_{pop}	50
sub-string length coding for each decision variable, l_i	32
crossover probability, P_{cross}	0.65
mutation probability, P_{mute}	0.002
spreading parameter, σ	0.075
exponent in sharing function, α	2.0
seed for random number generator, S_r	0.455

For the synthesis of MeOAc in SMBR, the decision variables can be classified as (a) fixed cost parameters [total number of columns (N_{col}), and length (L_{col}) and diameter (d_{col}) of each column]; (b) operating cost parameters [temperature (T), eluent flow rate (γ), and maximum flow rate in section P (Q_p), which is related to the maximum pressure drop in the system]; (c) throughput parameters [feed flow rate (α) and product flow rate at the raffinate port (β)]; and (d) process parameters [switching time (t_s) and distribution of number of columns in sections P, Q, R, and S (p, q, r, s)]. In this paper, we considered few multiobjective optimization problems associated with both existing and design stage. The Pareto optimal solutions are obtained using NSGA.[14] Table 1 lists the numerical parameter values used in NSGA in all the optimization runs. In all the optimization runs presented in this paper, 50 chromosomes (solutions) were considered, and results are presented after 50 generations (iterations). The CPU time taken to generate one Pareto set is about 7 min on a Cray J916 supercomputer. It should be noted that one simulation run is considered to be one when cyclic

Table 2. Description of the Multiobjective Optimization Problems Solved Together: Constraints, Bounds of Decision Variables, and Fixed Parameters

case	objective function	constraint	decision variables	fixed parameters
1: existing	max Y_{MeOAc} max P_{MeOAc}	$Y_{MeOAc} \geq 80\%$ $P_{MeOAc} \geq 90\%$	$5 \leq t_s \leq 40$ min $1 \leq \gamma \leq 4$	$\alpha = 0.2$, $\beta = 1.0$, $Q_p = 1$ mL/min, $T = 318$ K $L_{col} = 25$ cm, $d_{col} = 0.94$ cm, $N_{col} = 4$ $p = q = r = s = 1$, $C_{HOAc,f} = 2$ mol/L
1a: existing variable α	max Y_{MeOAc} max P_{MeOAc}	$Y_{MeOAc} \geq 80\%$ $P_{MeOAc} \geq 90\%$	$1 \times 10^{-5} \leq \alpha_1, \alpha_2, \alpha_3 \leq 0.5$	same as case 1 except $\gamma = 3.79$, $t_s = 18$ min, $\alpha_4 = 4\alpha - (\alpha_1 + \alpha_2 + \alpha_3)$
2: design stage	min γ min V_{solid}	$Y_{MeOAc} \geq 80\%$ $P_{MeOAc} \geq 98\%$	$1 \leq t_s \leq 40$ min $0.8 \leq \gamma \leq 4$ $10 \leq L \leq 150$ cm χ	$\alpha = 0.1$, $\beta = 0.6$, $Q_p = 2$ mL/min, $T = 318$ K $d_{col} = 0.94$ cm, $C_{HOAc,f} = 2$ mol/L $N_{col} = 4$, 5 or 6
3: existing	max Y_{MeOAc} max P_{MeOAc} min γ	$Y_{MeOAc} \geq 80\%$ $P_{MeOAc} \geq 80\%$	$1 \leq t_s \leq 20$ min $\leq \beta \leq 0.9$ $1 \leq \gamma \leq 4$ χ	$\alpha = 0.1$, $Q_p = 2$ mL/min, $T = 318$ K $N_{col} = 5$, $L_{col} = 10$ cm, $d_{col} = 0.94$ cm, $C_{HOAc,f} = 2$ mol/L

steady-state has reached, which for this system is about 60 switching.

Case 1. Existing Setup: Maximization of Purity and Yield of Methyl Acetate

In this section, the optimal operating parameters using were determined corresponding to simultaneous maximization of purity and yield of methyl acetate ester for an existing setup. Thereafter, experiments were performed at the optimal operating conditions to verify the performance predicted by the optimization package. The optimization problem is described mathematically (see Table 2, case 1) as

$$\text{maximize } I_1 = P_{MeOAc}(t_s, \gamma) \tag{6a}$$

$$\text{maximize } I_2 = Y_{MeOAc}(t_s, \gamma) \tag{6b}$$

Subject to

$$P_{MeOAc} \geq 90\%;\ Y_{MeOAc} \geq 80\% \tag{7}$$

$$5\ (\text{min}) \leq t_s \leq 40\ (\text{min});\ 1 \leq \gamma \leq 4 \tag{8}$$

$$Q_p = 1\ \text{mL/min};\ \alpha = 0.2;\ \beta = 1;\ C_{HOAc}^{\ feed} = 2\ \text{mol/L} \tag{9a}$$

$$L = 25\ \text{cm};\ d_{col} = 0.94\ \text{cm};\ N_{col} = 4,\ p = q = r = s = 1 \tag{9b}$$

The choice of the two objective functions, I_1 and I_2, in eq 6 enable the simultaneous maximization of yield and purity of the desired product, MeOAc. These two objective functions were chosen, as the primary goal of MeOAc synthesis in SMBR are to maximize yield and purity (or selectivity) of MeOAc. Two constraints (eq 7) were used to ensure that yield and purity of MeOAc is greater than 80%. The direct esterification reaction is not severely equilibrium limited,[5] as the equilibrium conversion of acetic acid in a nonseparative reactor can reach as high as 98.5% at 318 K when the feed concentration of HOAc is 2 mol/L and methanol is in large excess (see Table 5). In SMBR, even higher conversion can be achieved if the operating conditions are set properly.[6] Two decision variables (eq 8) were used for case 1 optimization study. These are switching time (t_s) and the eluent flow rate (γ) since in sensitivity analysis[6] it was found that these two parameters are most influential. All other parameter values are kept fixed as shown in eq 9.

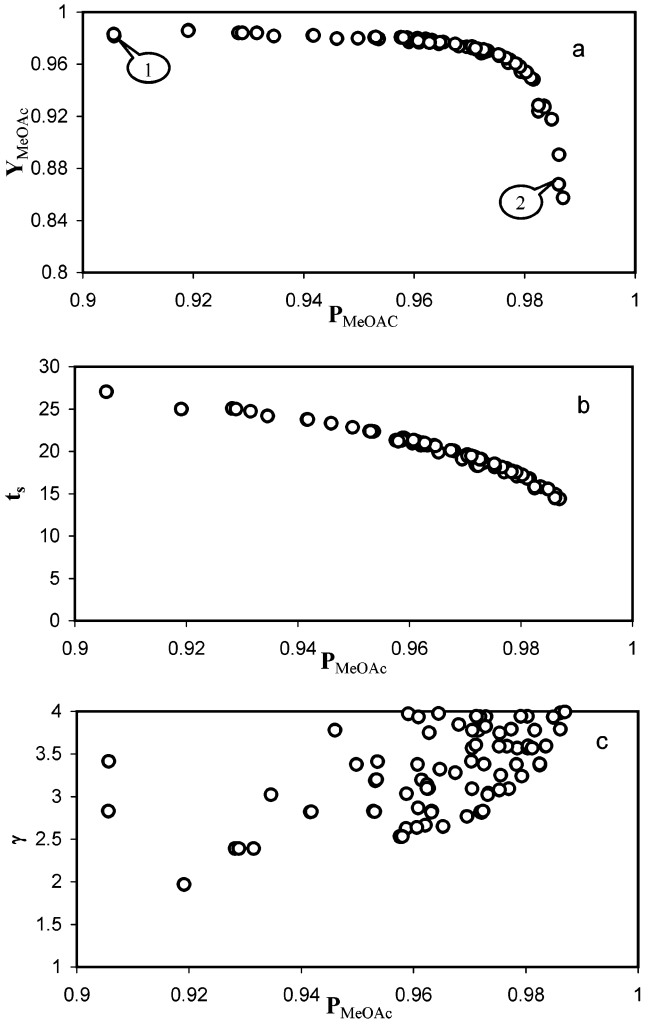

Figure 2. Optimal solutions and corresponding operating variables for maximization of purity and yield of MeOAc (case 1).

The Pareto optimal solutions in terms of maximizing purity and yield of MeOAc and the corresponding operating variables are shown in Figure 2. It was found that if purity of MeOAc improves, yield of MeOAc deteriorates and switching time (Figure 2b) plays the key role in determining the optimal solutions. For example, one can be achieved Y_{MeOAc} as high as 0.983 with P_{MeOAc} equal to 0.905 while P_{MeOAc} can be obtained as high as 0.986 with Y_{MeOAc} equal to 0.857. This could

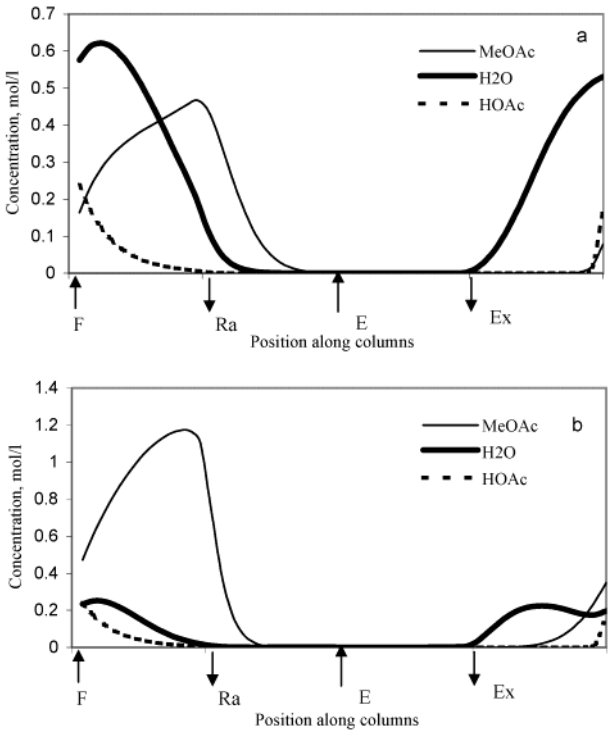

Figure 3. Concentration profiles of MeOAc−H_2O−HOAc at the end of 60 switching: (a) profiles corresponding to point 1 and (b) profiles corresponding to point 2 in Figure 2a.

be achieved by altering switching time (t_s) and eluent flow rate (γ) from, respectively, 27 min and 2.82 to 14.37 min and 3.99. The results can be explained (see Figure 3) by comparing the concentration profiles of the two different optimal points shown in the Pareto sets in Figure 2. It is obvious that when switching time increases, water (strongly adsorbed component) will break through from section P (feed section) contaminating the raffinate stream, leading to lower purity of ester, but on the other hand, longer switching time seems to be beneficial for the performance of section S, which is responsible for desorbing MeOAc, so that most of the ester and un-reacted acid can be recycled to section P at the end of a switching period, resulting in higher yield. Likewise, when switching time decreases, water is retained in section P resulting in higher P_{MeOAc}. The decrease of switching time deteriorates the performance of section S, as more ester and unreacted acid tend to be retained in section S and they appear at the extract port instead of the raffinate port during the next switching period, since section S becomes section R after the switch. Therefore, lower Y_{MeOAc} is expected. Figure 2c reveals that the eluent flow rate (γ) has less significant effect on the performance of the process, as it is sufficiently large for the complete regeneration of the adsorbent.

Experiments were carried out at optimal operating conditions corresponding to five optimal points in the Pareto set shown in Figure 2. Table 3 compares the experimental results with that of the optimal solutions. It was found out that optimal predicted solution could be achieved experimentally except when optimal P_{MeOAc} is very high (points 4 and 5). This is in agreement with our earlier study[6] of the effect of switching time on the performance of SMBR. It was found that the experimental results deviate from the model predictions when switching time is small. This is presumably due to the nonlinear behavior (long tail) of the water (strongly adsorbed component) concentration front toward the resin. At low switching time, there is not enough time for complete regeneration of the solid adsorbent. Hence, water breaks through at the product port in the next cycle thereby lowering the purity value obtained experimentally. This certainly can be improved if competitive nonlinear adsorption is used in the model. To verify that incomplete regeneration of the solid adsorbent is the cause for lower P_{MeOAc}, an experiment was repeated with identical conditions as that of point 5 (Table 3) except at a higher γ value. When γ was increased from 3.79 (set no. 5) to 5.0 (set no. 5a), P_{MeOAc} increased from 0.935 to 0.961 (see Table 3).

Table 3. Comparison of Optimal Predictions with Experimental Results[a]

			optimum solution		experimental results	
set no.	t_s (min)	g	P_{MeOAc}	Y_{MeOAc}	P_{MeOAc}	Y_{MeOAc}
1	25	2.98	0.921	0.982	0.930	0.983
2	21	3.13	0.965	0.976	0.959	0.982
3	18	3.79	0.977	0.963	0.971	0.967
4	15.5	3.43	0.981	0.931	0.946	0.952
5	14.5	3.79	0.986	0.868	0.935	0.904
5a	14.5	5.00	0.987	0.863	0.961	0.901

[a] Experimental conditions: $Q_p = 1$ mL/min; $\alpha = 0.2$; $\beta = 1$; $C_{HOAc}^{feed} = 2$ mol/L, $L = 25$ cm; $d_{col} = 0.94$ cm; $N_{col} = 4$, $p = q = r = s = 1$.

Case 1a: Effect of Distributed Feed

One of the limitations of the SMB is that during much of the operation the stationary phase in some of the columns are either completely free of solutes or contains only product so that the separation capacity is significantly reduced. One way to improve SMB efficiency is to use nonsynchronous switching like in the Varicol[17] process. An alternative option that could improve the effective utilization of adsorbent phase would be to vary the feed flow rate during a global switching interval. Recently, Zhang et al.[18] applied a similar concept, which they named as PowerFeed, to one of our previously studied[19] systems, separation of chiral drugs. To evaluate the efficacy of this approach, and to determine the extent the performance of SMBR could be improved by using variable (distributed) feed flow rate, the following optimization problem for the SMBR with four sub-feed interval was formulated and solved:

$$\text{maximize } I_1 = P_{MeOAC}(\alpha_1, \alpha_2, \alpha_3) \quad (10a)$$

$$\text{maximize } I_2 = Y_{MeOAc}(\alpha_1, \alpha_2, \alpha_3) \quad (10b)$$

Subject to

$$P_{MeOAC} \geq 90\%;\ Y_{MeOAC} \geq 80\% \quad (11)$$

$$1 \times 10^{-5} \leq \alpha_1, \alpha_2, \alpha_3 \leq 0.5 \quad (12a)$$

$$\alpha_4 = 4\alpha - (\alpha_1 + \alpha_2 + \alpha_3) \quad (12b)$$

$$Q_p = 1 \text{ mL/min};\ t_s = 18 \text{ min};\ \alpha = 0.2;\ \beta = 1;\ \gamma = 3.79;\ C_{HOAc}^{feed} = 2 \text{ mol/L} \quad (13a)$$

$$L = 25 \text{ cm};\ d_{col} = 0.94 \text{ cm};\ N_{col} = 4;\ p = q = r = s = 1 \quad (13b)$$

The operating conditions for the above problem are identical to the optimum solution obtained correspond-

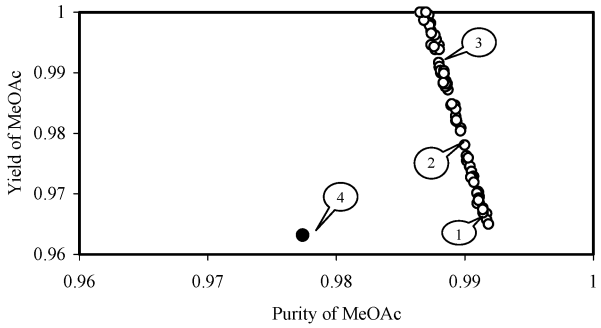

Figure 4. Comparison of optimal solutions for constant and variable (distributed) feed flow rate (case 1a): ●, constant feed; ○, variable feed.

ing to set number 3 in Table 2 except that the feed flow rate was not kept constant at $\alpha = 0.2$ for the entire switching interval and instead allowed to vary according to eq 12a. Equation 12b is used to ensure that total feed flow rate is same as that of the constant feed flow case (set 3 in Table 3), and therefore, the optimum results can be compared. Figure 4 compares the optimal solution, and it is evident from the figure that by varying (distributing) the feed flow rate (keeping the total feed flow rate constant), both the purity and yield of MeOAc can be improved. Table 4 compares the objective function values and the corresponding optimal feed flow rates at the four time intervals for three optimal points with the reference point 4 (same as set 3 listed in Table 3) shown in Figure 5. It was observed that the distribution of the feed flow rate for all the optimal solutions represents a uniform cyclic (periodic) behavior. The feed flow rate (α_1) is extremely small during the first subinterval, increases to a higher value for the second and the third time interval, and finally decreases to a lower value at the last time interval. The advantage of

Table 4. Comparison of Objective Function Values for Constant and Variable Feed Flow Rate

point in Figure 4	P_{MeOAc} (%)	Y_{MeOAc} (%)	α_1	α_2	α_3	α_4
1	99.1	96.7	9.0×10^{-4}	0.198	0.397	0.204
2	99.0	98.1	6.0×10^{-5}	0.256	0.399	0.146
3	98.8	99.2	2.0×10^{-4}	0.338	0.400	0.0623
4	97.7	96.3		$\alpha = 0.2$		

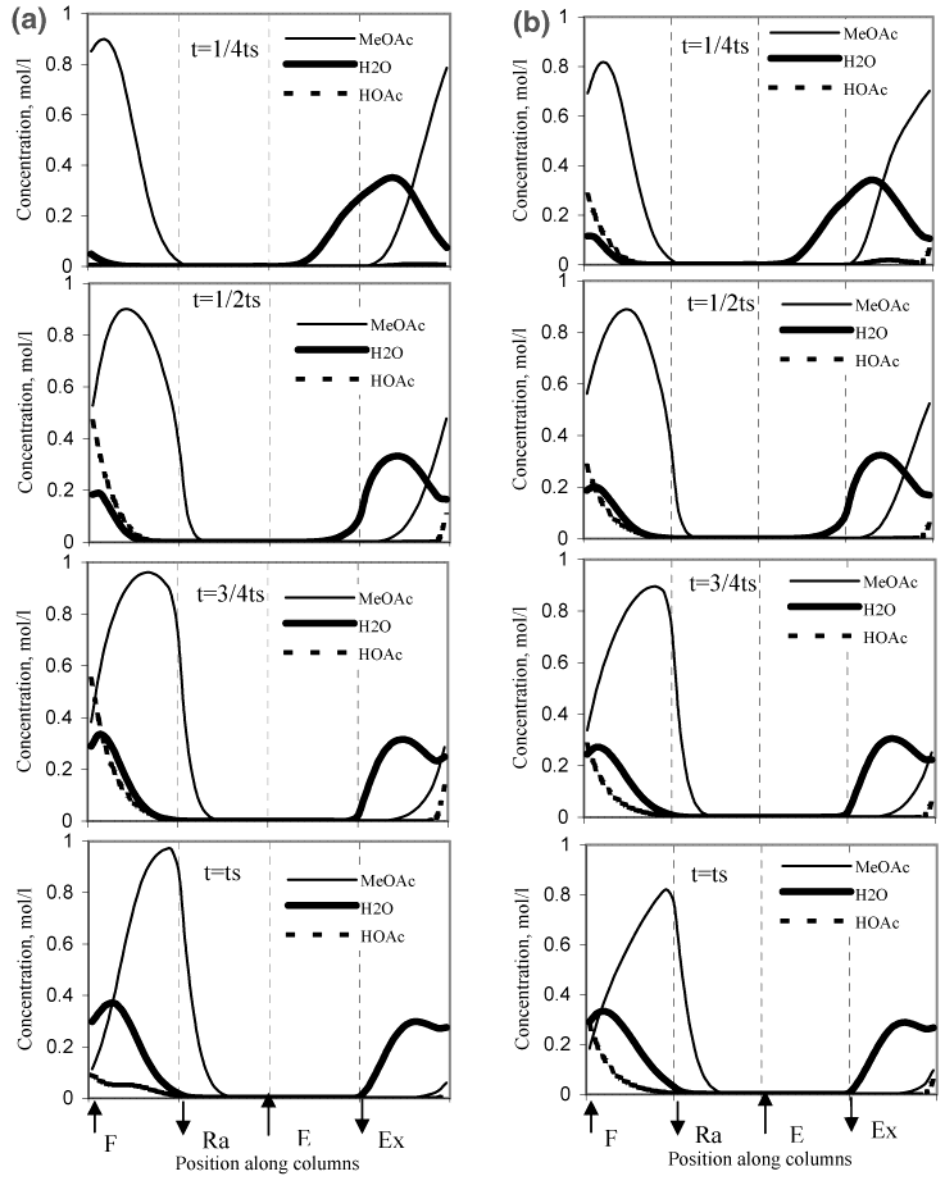

Figure 5. Concentration profiles of MeOAc−H_2O−HOAc for constant and variable feed at the end of sub-time intervals after cyclic steady states have been reached: (a) variable feed (point 3) and (b) constant feed (point 4) in Figure 4.

this particular cyclic behavior for the performance of SMBR can be illustrated by comparing the concentration profiles for constant (point 4 in Table 4) and variable (point 3 in Table 4) feed flow rate at the end of each of the four sub-time intervals as shown in Figure 5. The figure shows that the concentration front of water moves faster toward the raffinate port and tends to break through from section P during the last time interval when the feed flow rate is constant. This gives rise to lower purity of ester (P_{MeOAc}) compared to variable feed flow. Likewise, the smaller feed flow rates in the first and last time interval help to improve the yield of ester (Y_{MeOAc}). Since Q_p is fixed, the flow rate in section S [$Q_s \equiv (1 - \alpha)Q_P$] increases as the feed flow rate (α_1 and α_4) decreases and the performance of section S becomes better, which leads to higher yield as discussed earlier. The forced periodic feed flow rate could improve the performance SMB for other operating conditions also, and the extent improvement vary depending on the specific reaction system, column configuration, and numbers of subtime intervals employed. Similarly, one can use forced periodic eluent flow rate to improve Y_{MeOAc} and P_{MeOAc} compared to fixed total eluent flow rate or for a fixed value of Y_{MeOAc} and P_{MeOAc} can minimize total eluent flow rate compared to constant eluent flow rate. However, for the synthesis of MeOAc it was observed that effect of variable eluent flow rate (γ) is less significant compared to variable feed flow rate (α).

Case 2. Design Stage Optimization: Minimization of V_{solid} and γ

The performance of reactive SMB process was next optimized at the design-stage. Since adsorbent requirement and eluent consumption are usually the key factors to decide the capital (fixed) and operating cost of a SMBR plant, it is worth considering such a problem in which desired goal is to obtain specified purity and yield of MeOAc with minimal eluent flow (γ) and adsorbent requirement (V_{solid}). The optimization was carried out to determine the optimal column length for a 4-, 5-, or 6-cloumn SMB unit. In this case, in addition to t_s and γ, two other decision variables were incorporated, namely, length of each column, L_{col}, and column configuration (χ). The symbol χ indicates number of columns in respective sections. For example, χ = 2/1/1/2 means there are 2 columns in sections P and S while only one column in sections Q and R (see Figure 1). The detailed optimization formulation is described in Table 2, case 2. To obtain a smooth Pareto within reasonable computation time, we intentionally increased the constraint for purity requirement of MeOAc to a higher value of 98%.

The Pareto optimal solutions obtained for the SMBR systems for different N_{col} values are illustrated in Figure 6a. It can be observed that 6-column SMBR requires the least amount of adsorbent and eluent for the desired task of obtaining more that 98% purity and 80% yield of MeOAc. The 6-column SMBR performs better than a 4- and 5-column SMBR in terms of demanding less amount of adsorbent at similar eluent flow rate or less eluent for same total V_{solid}. The increased flexibility with larger number of columns leads to better utilization of the stationary phase. The flexibility of introducing more columns into the reactive sections (P and S) allows choosing lower optimum column length to achieve the same product purity. Moreover, the increase of the

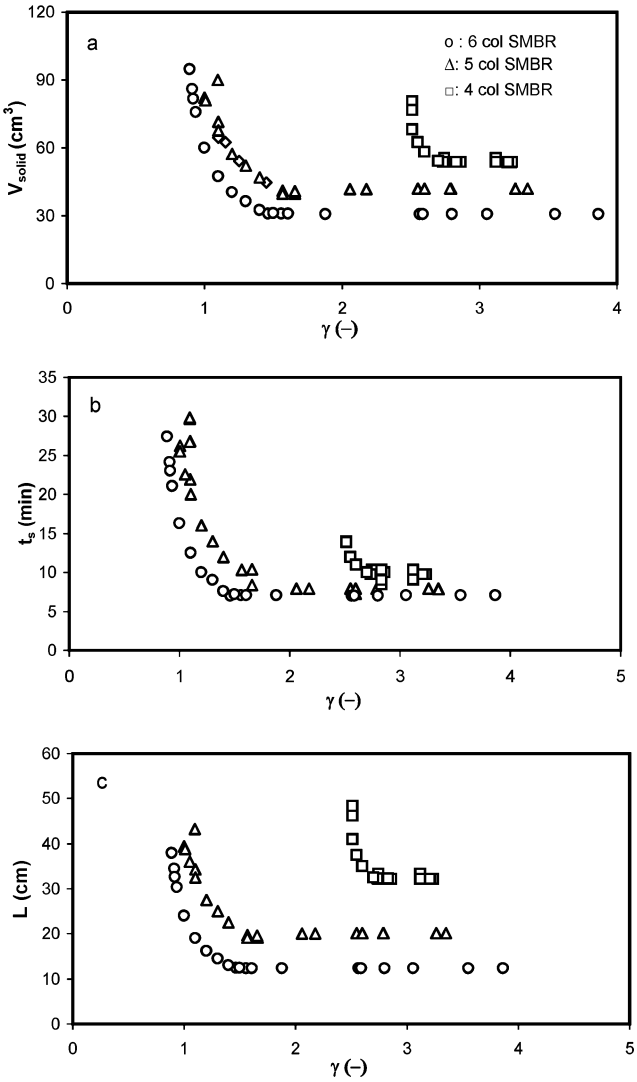

Figure 6. Optimal solutions for minimization of adsorbent volume and eluent consumption and corresponding decision variables (case 2).

number of columns in SMBR setup leads to establishment of true moving bed behavior and hence the improvement in performance. The optimum column configuration (χ) of 5- and 6-column SMBR is 2/1/1/1 and 3/1/1/1, respectively. The corresponding switching time and column length are shown in parts b and c, respectively, of Figure 6.

Case 3. Maximization of Y_{MeOAc} and P_{MeOAc} and Minimization of γ

So far, we focused on optimizing two objective functions simultaneously. However, the operation of SMBR is considerably influenced by quite a number of operating parameters, and sometimes it is not sufficient if one tries to optimize only two objective functions concurrently. Hence, solving a triple optimization problem may be a better approach to provide further insight into the design and operation of a reactive SMB process. In this section, a typical triple optimization problem in terms of maximization of purity and yield of MeOAc together with the minimization of eluent consumption was considered for a 5-column reactive SMB unit. The length of each column (L_{col}) was fixed at 10 cm based on our earlier studies.[17] The mathematical formulation of the

Table 5. Adsorption Constant, K_i, Kinetic Parameters, k_f, K_e, and n, and Dispersion Coefficients, D_i

T (K)	K_{MeOAc}	K_{H_2O}	K_{HOAc}	k_f (min^{-1})	K_e (mol/L)	$10^6 D_{MeOAc}$ (m^2/s)	$10^6 D_{MeOH}$ (m^2/s)	X_{HOAc}[a]
313	0.400	3.078	0.480	0.850	348.596	5.006	14.583	0.986
318	0.376	2.938	0.425	1.062	334.023	3.884	11.168	0.985
323	0.359	2.781	0.380	1.438	325.261	3.459	11.029	0.984

[a] Equilibrium conversion based on $C_{HOAc}^{feed} = 2.0$ mol/L and excess methanol.

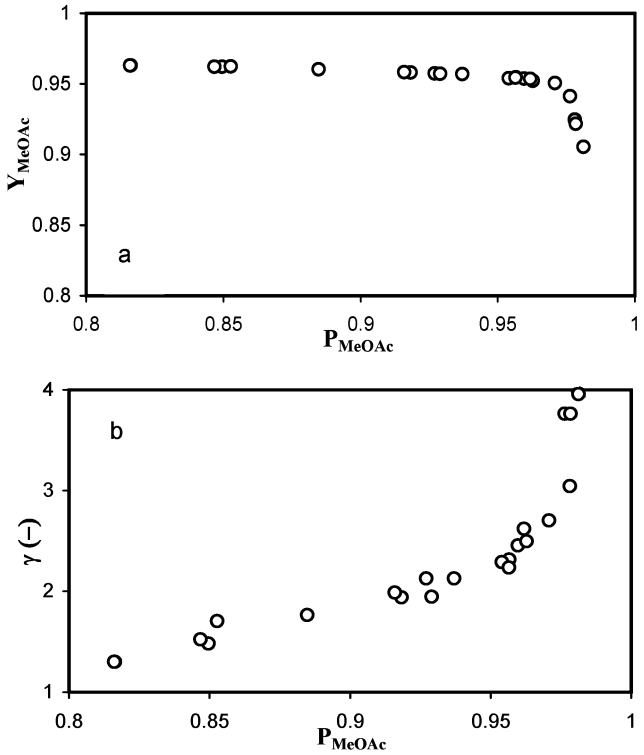

Figure 7. Pareto optimal solutions for triple objective function optimization (case 3).

problem is described in Table 2 as case 3. For the convenience of analysis, the Pareto solutions are plotted in two dimensions. Figure 7a shows that Y_{MeOAc} decreases as P_{MeOAc} increases, while Figure 7b illustrates that increase of P_{MeOAc} is at the cost of more eluent consumption. One can move for optimal values of (P_{MeOAc}, Y_{MeOAc}, γ) from (0.816, 0.963, 1.302) to (0.954, 0.954, 2.292) to (0.981, 0.905, 3.957). The optimal column distribution for reactive SMB was $\chi = 2/1/1/1$.

Conclusions

The multiobjective optimization of reactive SMB for the synthesis of MeOAc was performed using an adaptation of genetic algorithm, NSGA. The optimal solutions in terms of maximization of purity and yield of MeOAc for the existing experimental setup were confirmed with the experimental results by running the unit at the optimal operating conditions. This experimental verification not only demonstrated that the model is robust but also showed that optimization results can be duplicated experimentally. To further improve the reactor performance, the feed flow rate was varied during a global switching period, and it was found that both the purity and yield of MeOAc could be improved compared to the constant feed flow process. Two other multiobjective optimization studies were performed; one in which fixed and operating cost related parameters were minimized while in the other a more meaningful triple objective function optimization was solved. This paper illustrates a realistic approach toward the optimal design and operation of reactive SMB systems.

Acknowledgment

This work was supported by an Academic Research Grant of the National University of Singapore. One of the authors (A.K.R.) acknowledges Professor S. K. Gupta of the Indian Institute of Technology, Kanpur, who introduced the exciting field of multiobjective optimization using genetic algorithm while he was visiting the National University of Singapore in 1999.

Appendix: Complete Set of Equations for the Mathematical Model Used in This Work and Described in Detail Elsewhere[6]

Material balance

$$\frac{\partial C_{ij}^{(N)}}{\partial t} + \left(\frac{1-\epsilon}{\epsilon}\right)\frac{\partial q_{ij}^{(N)}}{\partial t} + \frac{u_\phi}{\epsilon}\frac{\partial C_{ij}^{(N)}}{\partial z} - \left(\frac{1-\epsilon}{\epsilon}\right)\nu_i R_j^{(N)} = D_i \frac{\partial^2 C_{ij}^{(N)}}{\partial z^2} \quad \text{(A1)}$$

for the component i in the jth column during the Nth switching period, where i = HOAc, MeOAc or H_2O, u_ϕ designate superficial flow rate in section ϕ (where $\phi = P, Q, R, S$), and the reaction rate and adsorption isotherm are given by

$$q_{ij}^{(N)} = k_f\left[q_{HOAc,j}^{(N)} - \frac{q_{MeOAc,j}^{(N)} q_{H_2O,j}^{(N)}}{K_e}\right] \quad \text{(A2)}$$

$$q_{ij}^{(N)} = K_i C_{ij}^{(N)} \quad \text{(A3)}$$

The initial and boundary conditions are given by Initial condition:

$$\text{When } N = 0,\ C_{ij}^{(0)} = c_{ij}^{initial} = 0 \quad \text{(A4)}$$

When $N \geq 1$

$$C_{ij}^{(N)} = C_{i,j+1}^{(N-1)} \quad \text{for} \quad j = 1 \sim (N_{col} - 1) \quad \text{(A5)}$$

$$C_{ij}^{(N)} = C_{i1}^{(N-1)} \quad \text{for} \quad j = N_{col} \quad \text{(A6)}$$

Boundary conditions: Feed entry point (point A in Figure 1)

$$C_{i1}^{(N)}|_{z=0} = (1-\alpha)C_{i,Ncol}^{(N)}|_{z=L} + \alpha C_{i,f} \quad \text{(A7)}$$

Raffinate takeoff point (point B in Figure 1)

$$C_{i,p+1}^{(N)}|_{z=0} = C_{i,p}^{(N)}|_{z=L} \quad \text{(A8)}$$

Eluent inlet point (point C in Figure 1)

$$C_{i,p+q+1}^{(N)}|_{z=0} = \left[\frac{1-\beta}{1-\beta+\gamma}\right] C_{i,p+q}^{(N)}|_{z=L} \qquad \text{(A9)}$$

Extract takeoff point (point D in Figure 1)

$$C_{i,p+q+r+1}^{(N)}|_{z=0} = C_{i,p+q+r}^{(N)}|_{z=L} \qquad \text{(A10)}$$

The mass balance equation (eq A1), initial (eqs A4−A6) and boundary conditions (eqs A7−A10), kinetic equation (eq A2), and adsorption isotherm (eq A3) completely define the SMBR system. After each switching, column numbering was redefined according to equation A11 so that feed is always introduced into the first column (Table 5).

before switching	after switching
column 1	column N_{col}
column j	column $j-1$ $\quad j = 2, 3, ..., N_{col}$

(A11)

Notation

C = liquid-phase concentration, mol/L
d = diameter of the column, m
L = length of column, m
N = number of switching, total number of columns
p = number of columns in section P
P = purity, section P
q = number of columns in section Q
Q = volume flow rate, cm^3/min, section Q
r = number of columns in section R
R = section R
s = number of columns in section S
S = section S
t = time, min
V = volume of solid, cm^3
X = conversion
Y = yield
z = axial coordinate, cm

Greek Letters

α = fraction of feed
β = fraction of raffinate
γ = fraction of eluent
ϵ = void fraction

Subscripts/Superscripts

col = column
E = eluent
F = feed
HOAc = acetic acid
MeOAc = methyl acetate
p = section P
q = section Q
r = section R
R = raffinate
s = switching, section S

Literature Cited

(1) Broughton, D. B.; Gerhold, C. G. US Patent 6136198, 1961.

(2) Ray, A.; Tonkovich, A.; Carr, R. W.; Aris, R. The simulated countercurrent moving bed chromatographic reactor. *Chem. Eng. Sci.* **1990**, *45*, 2431.

(3) Ray, A. K.; Carr, R. W.; Aris, R. The simulated countercurrent moving bed chromatographic reactor: A novel reactor-separator. *Chem. Eng. Sci.* **1994**, *49*, 469.

(4) Ray, A. K.; Carr, R. W. Experimental study of a laboratory scale simulated countercurrent moving bed chromatographic reactor. *Chem. Eng. Sci.* **1995**, *50*, 2195.

(5) Yu, W.; Hidajat, K.; Ray, A. K. Determination of adsorption and kinetic parameters for methyl acetate esterification and hydrolysis reaction catalyzed by Amberlyst 15. *Appl. Catal. A: Gen.* **2003**, in press.

(6) Yu, W.; Hidajat, K.; Ray, A. K. Modeling, simulation and experimental verification of methyl acetate synthesis in simulated moving bed reactor, revised version submitted to *Ind. Eng. Chem. Res.* **2003**, *42*, 6743−6754.

(7) Migliorini, C.; Fillinger, M.; Mazzotti, M.; Morbidelli, M. Analysis of simulated moving bed reactors. *Chem. Eng. Sci.* **1999**, *54*, 2475.

(8) Dunnebier, G.; Fricke, J.; Klatt, K. Optimal design and operation of simulated moving bed chromatographic reactors. *Ind. Eng. Chem. Res.* **2000**, *39*, 2290.

(9) Lode, F.; Houmard, M.; Migliorini, C.; Mazzotti, M.; Morbidelli, M. Continuous reactive chromatography. *Chem. Eng. Sci.* **2001**, *56*, 269.

(10) Azevedo, D. C. S.; Rodrigues, A. E. Design methodology and operation of a simulated moving bed reactor for the inversion of sucrose and glucose-fructose separation. *Chem. Eng. Sci.* **2001**, *82*, 95.

(11) Bhaskar, V.; Gupta, S. K.; Ray, A. K. Applications of multi-objective optimization in chemical engineering. *Rev. Chem. Eng.* **2000**, *16*, 1.

(12) Deb, K. *Multi-objective optimization using evolutionary algorithms*; John Wiley & Sons: New York, 2001.

(13) Coello, C. C. A.; Van Veldhuizen, D. A.; Lamont, G. B. *Evolutionary algorithms for solving multi-objective problems*; Kluwer Academic Publishers: New York, 2002.

(14) Nandasana, A. D.; Ray, A. K.; Gupta, S. K. Applications of the nondominated sorting genetic algorithm (NSGA) in chemical reaction engineering. *Int. J. Chem. Reactor Eng.* **2003**, *1*, R2.

(15) Goldberg, D. E. *Genetic Algorithms in Search, Optimization and Machine Learning*; Addison-Wesley Publishing Co.: Reading, MA, 1989.

(16) Schiesser, W. E. *The Numerical Method of Lines*; Academic Press: New York, 1991.

(17) Yu, W.; Hidajat, K.; Ray, A. K. Optimal operation of reactive simulated moving bed and Varicol systems. *J. Chem. Technol. Biotechnol.* **2003**, *78*, 287.

(18) Zhang, Z.; Mazzotti, M.; Morbidelli, M. PowerFeed operation of simulated moving bed units: changing flow-rates during the switching interval. *J. Chromatogr. A* **2003**, *1006*, 87.

(19) Zhang, Z.; Hidajat, K.; Ray, A. K.; Morbidelli, M. Multi-objective optimization of SMB and Varicol process for chiral separation. *AIChE* **2002**, *48*, 2800.

Received for review May 6, 2003
Revised manuscript received September 29, 2003
Accepted October 15, 2003

IE030387P